Ocean Mixing: Oxford Encyclopedia.

Carl Wunsch*
Department of Earth and Planetary Sciences
Harvard University
Cambridge MA 02138
email: cwunsch@fas.harvard.edu

September 28, 2016

Summary

Oceanic mixing is one of the major determinants of the ocean circulation and its climatological influences. Existing distributions of mixing properties determine the rates of storage and redistribution within the climate system of fundamental scalar tracers including heat, freshwater, oxygen, carbon, and others. Observations have over-turned earlier concepts that mixing rates might be approximately uniform throughout the ocean volume, with profound implications for determining the circulation and its properties. Inferences about past and potential future oceanic circulations and the resulting climate influence require determination of changed energy inputs and the expected consequent adjustment of mixing processes and their influence.

Keywords

Mixing, stirring, balanced eddies, internal waves, oceanic general circulation, sub-mesoscale

Mixing and Stirring

The ocean stores, redistributes, and exchanges with the atmosphere a wide variety of substances essential to the climate system including heat (enthalpy), freshwater, kinetic and potential energies, carbon, oxygen, and nutrients of all sorts. An understanding of climate, and its past and

*Also, Dept. of Earth, Atmospheric and Planetary Sciences, MIT

potential future changes, thus requires a complete depiction of the distribution and redistribution of these scalar properties once they have entered the ocean. In other words, the oceanic general circulation in all of the elements that control it and change it must be described if varying climate states are to be understood.

In a laminar flow, physics dictate that the movement of scalar properties is cleanly divisible into advective components—proportional to the velocity field, $\mathbf{v}$, and diffusive ones dependent upon the molecular diffusion coefficients, κ, arising from the internal energy of the fluid. In a turbulent fluid like the ocean, the distinction is no longer clear-cut: the inability to analyze and cleanly represent the flow field from the largest scales down to the molecular ones has led historically to representations of the unresolved scales as, at least in part, as "diffusion-like." This situation renders the study of oceanic mixing processes as a subset of a combined laminar-turbulent fluid, but with the turbulence having the special properties of a rotating, stratified fluid shell with complex vertical and horizontal boundaries. A complete discussion of mixing encompasses the entirety of oceanic fluid physics including fully turbulent flows in the presence of stratification, rotation, external forcing, complex boundaries, and global-scale fluid flows. A systematic account of many of these elements can be found in the book by Thorpe (2005). Mixing is simultaneously a consequence of, and a cause of, the large-scale general circulation of the ocean.

Several important elements of ocean mixing have been clarified recently: (1) Processes and effective rates vary by three and four orders of magnitude over the ocean volume; (2) The physics of mixing is deeply intertwined with the oceanic energy budget; (3) All of the enormous range of scales of oceanic motions from 10,000 km to 1 mm are both affected by, and in turn influence, variations in mixing. The consequences have proven profound for basic understanding of the oceanic general circulation and its climate impacts. To limit this article, the focus is primarily on the interior ocean, touching only tangentially on the special regions of the mixed-layers at the sea-surface and sea floor, and the variety of boundary layers occurring over sidewalls and general topographic features. Most attention is paid to the vertical or "diapycnal" problem involving transfers across the stable stratification, and which differs fundamentally both in magnitude and physics from so-called isopycnal mixing—easier motions along layers of near-constant density—nearly perpendicular to local gravity.

Discussion of the causes and numerical values of mixing, apart from being an extremely challenging observational problem, is at the very edge of modelling and theoretical understanding of fluid physics. Much of the context of this discussion can be understood from the conventional advection-diffusion equation for a tracer, C, written for an ordinary fluid e.g.,

$$\frac{\partial C}{\partial t} + \mathbf{v}\cdot\nabla C = \kappa_C \nabla^2 C. \qquad (1) \quad \texttt{\{advectiondiff}$$

κ_C is a Newtonian diffusion coefficient of molecular origin, assumed constant in both space and time and ∇ is the three-dimensional gradient operator in any suitable coordinate system. The most common tracers in oceanic studies are temperature, T, and salinity, S. These two fields determine the density, ρ, structure of the ocean as

$$\rho(\mathbf{r},t) = \varrho(T(\mathbf{r},t), S(\mathbf{r},t), p(\mathbf{r},t)) \tag{2}$$ {density1}

where $\mathbf{r}$ is a three-dimensional position ((x,y,z) in Cartesian coordinates) and p is the pressure. (Variations in ρ are here considered to be "small" in the mass balance, but important in the momentum equations.) The function in Eq. (2) involves a complicated empirical rule rendering the density field a nonlinear function of the variables T, S, p. For many purposes, however, it can be linearized in the form,

$$\rho(\mathbf{r},t) = \rho_0 (1 - \alpha T(\mathbf{r},t) + \beta S(\mathbf{r},t) + \gamma p(\mathbf{r},t)), \tag{3}$$ {density2}

where ρ_0, α, β, γ are treated as locally constant. Often γ is set to 0, in the Boussinesq approximation, treating the fluid as incompressible. If Eq. (3) is adequate, ρ itself can be treated as a tracer, $C = \rho$.

In the simplest cases, $\mathbf{v}$, κ_C are independent of tracer concentration C (called a "passive" tracer), but if T, S, or ρ are being considered, they influence $\mathbf{v}$ ("active" tracers). Typical numerical values are $\kappa_C \approx 10^{-7}\mathrm{m}^2/\mathrm{s}$ for temperature and 10^{-9} m^2/s for salt. Discussion of tracer mixing in the ocean is intimately tied to momentum mixing (frictional processes) and they are best treated together. Thorpe (2007) has a clear introduction. For present purposes, $\mathbf{v}$ is taken as a "given."

The derivatives in the tracer "diffusion" term on the right-hand side only become important when the length scales over which they are taken become very small, of order centimeters or less. An attractive step for an oceanographer attempting to understand the behavior of a tracer in the ocean is to argue that this diffusion term can be neglected, setting the left-hand-side equal to zero so that,

$$\frac{\partial C}{\partial t} + \mathbf{v}\cdot\nabla C = \frac{\partial C}{\partial t} + \nabla\cdot(\mathbf{v}C) = 0, \quad \nabla\cdot\mathbf{v} = 0 \tag{4}$$ {advectiondiff

As with much of fluid dynamics, most interest and difficulty arises from the overall behavior of the advection-term, $\mathbf{v}\cdot\nabla C$. Estimates of the spatial variation of velocity, $\mathbf{v}$, show it carrying laminar-like structures on the largest scale (e.g., the overall gyre structure of the circulation of the Pacific Ocean) through an entire stochastic continuum of spatial scales down to 1 millimeter. As far as can be determined, no spatial scales are absent in the range between these rough limits (or in the jargon, there is no spatial "spectral gap"). Much, if not all, of the flow contains powerful random (stochastic) elements—that is, it is turbulent—and is best perceived from

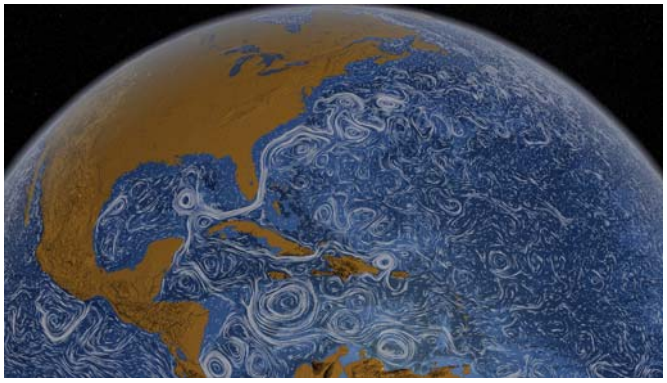

Figure 1: Surface speeds in part of the North Atlantic Ocean (from website http://www.nasa.gov/topics/earth/features/perpetual-ocean.html#.Vy0DIoSDFBd). from a numerical model. Most of these features are intensely time-dependent and can be seen in an animation at the same web location. Myriad yet-smaller scale features exist in the ocean that are invisible to the eye in such an overview and remain beyond existing computing capacities. {perpetual_oce

one of the many animations of the ocean circulation now available on the web. Fig. 1 shows a snapshot of estimated surface speed in the ocean. The visually conspicuous "swirling" flows carry tracer properties with them, stretching their boundaries out to enormous lengths. These motions are commonly referred to, somewhat vaguely, as the oceanic "mesoscale eddies", or "balanced eddies". The latter terminology emphasizes their tendency to satisfy near-geostrophic balance (dominated by the Earth's rotation) although at the shortest scales, below about 10km, they become significantly non-geostrophic and are then commonly labelled "sub-mesoscale" eddies. Below visual detection, molecular processes are also at work, preventing the structures from becoming arbitrarily elongated.

Suppose a patch of dye with a circumferential distance of order D_0 is introduced into such a flow in two-dimensions (Fig. 2). An the initial time, at the patch edge, ∇C, and hence $\kappa_C \nabla^2 C$, may not be negligible, but the initial $D = D_0$ is sufficiently small that an integral of the last term in Eq. (1)

$$\oint_{D=D_0} |\kappa_C \nabla^2 C| dD, \tag{5}$$ {integral1}

taken around its boundary, *is* negligible compared to other integrated term from Eq. (1)

Through time, the patch is stretched out, and extended in a tortuous pathway. Even in comparatively simple, non-turbulent flows, pathways commonly have a chaotic behavior (see e.g. Ottino, 1989). The boundary demarcating the edge of the path becomes extended in time, growing to values $D >> D_0$. At this boundary, the gradients, ∇C, are extremely large, and the integrals in Eq. (5) taken around the long boundary D are very important and cannot be

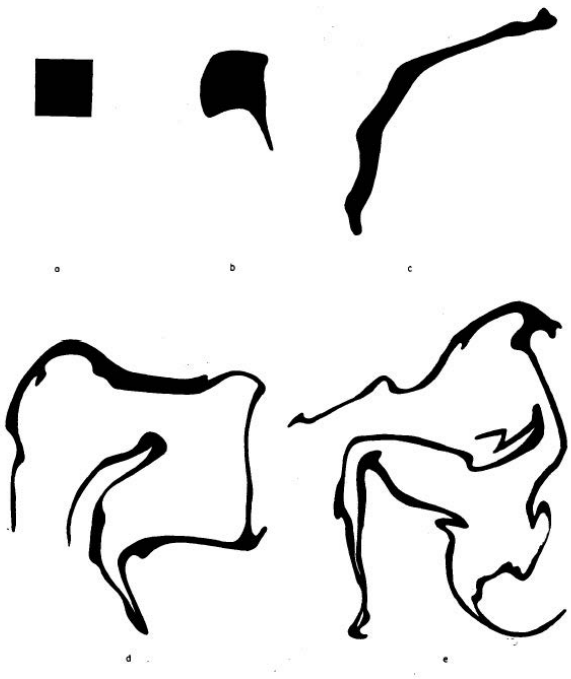

Figure 2: From Welander (1955) showing the "stirring" of a small square dye patch in a near two-dimensional fluid flow. "Mixing" would take place along the dye boundary which becomes greatly extended in length as time goes on. Molecular processes operate primarily at the dye-patch boundaries and ultimately limit the extensions of the patches. In three-dimensions the tendency to elongation is muted. {welander_1955

ignored and indeed prevent the fluid from developing arbitrarily elongated and tangled structures. Indefinite growth is prevented both by these molecular processes, and those acting to control particle separations within a dye patch (Salmon, 1998, Section 1.14). Thus one must distinguish the statistics of turbulent motion insofar as they affect the center of mass of the dye patch, from those controlling the separation of fluid particles within the patch (see especially, Garrett, 2006).

Eckart (1948) divided oceanic processes into three parts—supposing there exists a large-scale flow carrying tracer patterns of interest. Superimposed upon those large-scale, L, flows are smaller scale motions, L_s, which stretch the tracer out into the complex patterns with intricate and extended boundaries. He called those motions "stirring." Finally, the very smallest scales at both patch edges, and within the interior of the patch, the molecular scale l_m, rarely observed directly, are where molecular processes dominate and act to homogenize the fluid. (Note that Fig. 2 depicts an essentially two-dimensional fluid movement; in three dimensions the elongated, serpentine, structure is less-pronounced.)

Although the molecular scale was early on recognized as essential to understanding the

distribution of properties in the oceans, the observational tools available before about 1965 did not permit discussion of how these mixing processes actually operated. A great deal had been learned about the physics of conventional turbulence in unstratified, non-rotating fluids, but the oceanic applicability remained obscure. An oceanographic exception was the growth of interest in so-called double-diffusive processes, although most of that discussion was focussed on laboratory-scale experiments and theory (e.g., Radko, 2013).

For roughly the first 100 years of physical oceanography (to about 1965), observational capabilities on the largest scales were limited to ship-borne measurements of temperature and salinity, resulting in the now-familiar and classical charts of oceanic gyres and major boundary currents, and are known to be quasi-permanent features. These are identified with scale L, see Fig. 3, and which were and are represented as a large-scale, fundamentally laminar flow. On the other hand, oceanographers were well aware of the existence of smaller scales of flow (see Helland-Hansen and Nansen, 1909) and realized that they had both a dynamical and kinematical influences on the larger scales, ones that ultimately had to be treated statistically.

Assuming that these motions were turbulent, in the sense of being stochastic, and in a fluid-dynamics approach dating back to the 19th Century, it was hypothesized that both $\mathbf{v}$,C could be broken up into two pieces: $\mathbf{v} = \bar{\mathbf{v}} + \mathbf{v}'$, $C = \bar{C} + C'$, where the over-bar represents an averaging process, in space, or time, or both. If space was involved (a useful choice in a spatially homogeneous flow) the averaging interval was taken to be larger than the stirring scale L_s, but less than L, such that $\overline{\mathbf{v}'} = 0$, $\overline{C'} = 0$, but $\overline{\mathbf{v}'C'} \neq 0$. (See especially Tennekes and Lumley (1972) or any book on turbulence, e.g. Batchelor, 1953). Alternatively, the assumption might be made that a time average would remove all of the small scales—although that involves a strong and difficult-to-justify assumption about space-time statistics of the ocean. In particular, the longest available records do not support the existence of any kind of spectral gap in frequency. [1] Eq. (4) then becomes, when averaged,

$$\frac{\partial \bar{C}}{\partial t} + \bar{\mathbf{v}}\cdot\nabla\bar{C} + \nabla\cdot\overline{(\mathbf{v}'C')} = 0, \quad \nabla\cdot\mathbf{v}' = 0. \tag{6}$$

$\bar{\mathbf{v}}$,$\bar{C}$ are the quasi-laminar fields with everything else to be handled statistically. The problem—the "turbulence closure"—is what to do with the divergence of $\overline{\mathbf{v}'C'}$, the covariance of the

[1] Davis (1994) emphasized, absent a spatial or temporal gap in scales, the assumption that such mixed averages such as $\overline{\mathbf{v}'\bar{C}} = 0$ can fail. Few oceanic measurements exist such that averages taken over any long time-scale are truly stable: e.g., doubling the record length usually measurably changes the calculated averaged and which may well be covarying with the variability of the fluctuations. The trough in spectra at frequencies just below the inertial frequency (usually denoted f) is sometimes regarded as representing a spectral gap, but it is probably best regarded as the effect of a peak, rather than a minimum. Recent theoretical arguments have also shown how energy can be transferred across this frequency interval.

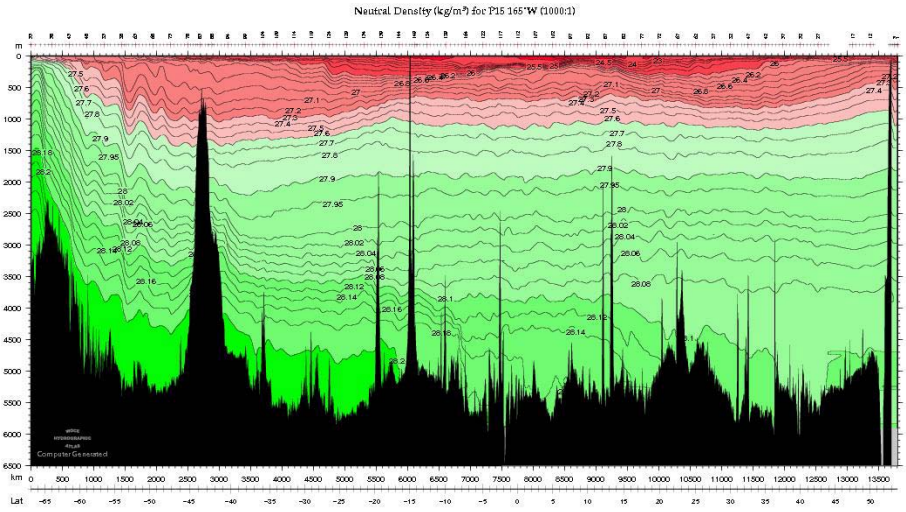

Figure 3: Neutral surfaces down the central Pacific Ocean (from the Pacific Atlas of the World Ocean Circulation Experiment, Talley et al., 2007). Note that the contouring interval is not uniform. The largest scales are quasi-stable over decades, whereas the visual much smaller scale variability was poorly understood until recently, and is best regarded as a mixture of geostrophically balanced motions and gravitationally governed internal waves. Surfaces above roughly 1000m in the Southern Ocean outcrop to the surface before they reach the Antarctic continent. These outcropping surfaces can be stirred and mixed by direct wind-action. At greater depths, surfaces away from the Southern Ocean are roughly horizontal sometimes leading to depictions as the result of one-dimensional, vertical, advection-diffusion balances. These surfaces reach the continent to the south where they become involved with the formation of very dense water (Antarctic Bottom Water) visible as the deep green plume at the bottom left. This water must ultimately be returned to the sea surface if the ocean is in a steady-state, through processes requiring work to mix the properties upward against gravity. The "thermocline" is the region near the surface of the most rapid density change (controlled largely by temperature). Such figures have a very great vertical exaggeration with the horizontal range being nearly 10,000 km and the vertical range being 6 km and thus the topographic and isopycnal slopes are in practice very small, but nonetheless extremely important in many locations. The structure of isopycnal surfaces is very similar to that of neutral surfaces. {woce_atlas_p1

spreading scales? (In conventional homogeneous, isotropic turbulence, this divergence vanishes.) Following Osborne Reynolds and many others, it can be supposed that these spreading scales act as an analogue of the suppressed diffusive ones—but operating entirely locally on the L-scale so that,

$$\nabla \cdot \left(\overline{\mathbf{v}'C'}\right) = -K\nabla^2 \bar{C}. \tag{7}$$

In a turbulent flow, it is often argued that all tracers are stirred by eddies at the same rate so that K would be appropriate for all C. Because of known anisotropies in oceanic flows and features, anisotropic rules were used,

$$\nabla \cdot \left(\overline{\mathbf{v}'C'}\right) = -K_{xx}\frac{\partial^2 \bar{C}}{\partial x^2} - K_{yy}\frac{\partial^2 \bar{C}}{\partial y^2} - K_{zz}\frac{\partial^2 \bar{C}}{\partial z^2} \tag{8}$$

(in a Cartesian system) or in the most general form,

$$\nabla \cdot \left(\overline{\mathbf{v}'C'}\right) = -\nabla \cdot \left(\mathbf{K}\nabla \bar{C}\right), \tag{9}$$ {tensor1}

where

$$\mathbf{K} = \left\{ \begin{array}{ccc} K_{xx} & K_{xy} & K_{xz} \\ K_{yx} & K_{yy} & K_{yz} \\ K_{zx} & K_{zy} & K_{zz} \end{array} \right\} = \left\{ \begin{array}{ccc} K_{11} & K_{12} & K_{13} \\ K_{21} & K_{22} & K_{23} \\ K_{31} & K_{32} & K_{33} \end{array} \right\}, \tag{10}$$ {tensor2}

has become a tensor (written above both in the special Cartesian and a more general index forms) with spatial or even temporal structure whose physical form must obey certain rules (e.g. Griffies, 2007, P.288+).

Use of these "eddy" coefficients (and their analogues for viscosity in the momentum equations) have had a long and useful history. Extensive discussions can be found in Defant (1961, P. 107+). In both analytic and numerical modelling, the symmetric elements of $\mathbf{K}$ destroy any gradients long before they reach the l_m scale, and thus function *implicitly* to dissipate tracer variance. That mixing depends only on the *local* properties of C has been assumed: for a contrasting approach, see Canuto et al. (2007). Anti-symmetric elements can act as stirring motions, increasing the gradients; see e.g. Griffies (2004) or Flierl and McGillicuddy (2007).

At the time of this writing, a major field experiment, Diapycnal and Isopycnal Mixing Experiment in the Southern Ocean (DIMES; Sheen et al., 2013), is underway to better understand the structure of $\mathbf{K}$, albeit the physics of the Southern Ocean flow are often untypical of the global ocean.

Isopycnals and Neutral Surfaces

Most of the ocean is stably stratified (Fig. 3), and the fluid has difficulty in moving tracers across that stratification, which requires work against gravity. In contrast, movement perpendicular to

gravity involves much less work and energy (except for internal viscous stresses), and substantial evidence supports the inference that usually $K_{33} << K_{11}, K_{22}$. In practice, the surfaces of constant density, $x_3 = \sigma(x_1, x_2)$ in many places deviate from the horizontal (Fig. 3 at the southern end), and the expression representing vertical diffusion can become inaccurate. K_{33} is better expressed as $K_{\sigma\sigma}$ (a "diapycnal" diffusion) and $K_{11,}K_{22}$ and the various cross-terms become expressions for diffusion along the isopycnal surfaces ("isopycnal" diffusion). Because the equation of state of seawater, representing the density as a function of temperature, salinity, pressure, and location, $\rho(T(x_1, x_2, x_3), S(s, x_2, x_3), p(x_1, x_2, x_3))$ is significantly non-linear, many authors replace isopycnals with "neutral surfaces" along which the work done against gravity by movement along the surfaces is minimal. To emphasize that the "vertical" coordinate will differ from the geocentric vertical, the coordinate system $(x, y, z) \rightarrow (x_1, x_2, x_3)$ where it is understood here that x_3 is normal to an isopycnal or neutral surface and is nonetheless sometimes most simply written as z. Terminology "isopycnal" will be used here without distinguishing the various representations of surfaces of minimal work against gravity. K_{33} becomes a "diapycnal" coefficient, and $K_{11,22}$ are "isopycnal" coefficients. Over much of the ocean, the distinction between the geodetic vertical and the isopycnal normal direction can be neglected, but the difference is crucial in regions of isopycnal slope as seen in Fig. 3 in the Southern Ocean. The non-linearity of the equation of state gives rise to a number of sometimes puzzling behaviors of mixed fluids under the rubrics of "cabbelling" and "thermobaricity." (For example, two fluid parcels with different temperature and salinity but the same density will, when mixed, have a different density. See e.g., McDougall and Garrett, 1992; Schanze and Schmitt, 2013.)

By definition, in an isopycnal coordinate system, mixing cannot move fluid parcels of different density across the reference surfaces, but that is not true of passive tracers. This distinguishing behavior leads to a lot of detailed complexity in numerical models of the ocean.

Scales

Oceanic flows do not occupy discretely separable spatial scales, L, L_S, l_m, but consist instead of a continuum of near-geostrophic global horizontal scale structures (basin and larger), changing significantly in time only slowly (many decades and longer); a geostrophically balanced eddy field, with spatial scales of a few hundred kilometers and changing over many months and longer; an internal-inertial wave field on spatial scales of tens of kilometers and changing over hours to days; a "sub-mesoscale" where rotation no longer dominates the eddies, and a small-scale turbulence with features of tens of meters to millimeters tending to be three-dimensionally isotropic, and changing over seconds to days. These motions overlap in a continuous occupation of frequency/wavenumber spaces. Derivatives of tracers and velocity, taken over the smallest

scales usually greatly exceed those taken on the largest scales.

A small extension of Eckart's (1948) schematic description of oceanic mixing is that tracers varying on scale L are stirred by the balanced (geostrophic) and sub-mesoscale eddies (scale L_{BE}). Then localized breaking by the internal wave field (L_{IW}) generates the turbulence that is dissipated in a traditional turbulent cascade to the molecular scale l_m, dominating the final conversion into molecular scales. Although a useful conceptual structure, it can be very inaccurate and misleading. For example, the gyre scales contain many features such as the western boundary currents, the equatorial current system, etc. which lie on the same scale (order 100km) as do the balanced eddies. Balanced eddies appear to exist even at very long periods—much longer than a year. They include such diverse physics as linear and non-linear Rossby and Kelvin waves, isolated vortices, coupled waves, instability structures, etc. Internal waves overlap the high wavenumber part of the submesoscale eddy field, and also contain balanced "vortical" structures. This listing remains only a sketch, ignoring many different boundary layer types at the surface, sidewalls and bottom. All of these physical processes are coupled to a greater or lesser degree. Sometimes, as in resonant interactions of wave-like motions, energy can move from one space- and time-scale to radically different ones. In conventional turbulence, interactions take place only between nearest-neighbor wavenumber scales, leading to the discussion of power laws, of which the Kolmogoroff $k^{-5/3}$ law is the best known, and where energy "cascades" from large to smallest scales. But in the ocean, some processes produce cascades in the opposite direction with differing power laws. Wave-like motions are often invoked statistically in a "wave-turbulence" approach (e.g., Polzin and Lvov, 2011).

Generalizing, $K_{1j}, K_{2j}, K_{j1}, K_{j2}$ are dominated by the balanced eddies in the open ocean, with the submesoscale becoming most important where isopycnal slopes are steep. K_{33}, K_{3j}, K_{j3} are usually controlled by breaking internal waves and provides the ultimate link between the stirring-dominated isopycnal terms and the ultimate dissipation. Generalizations about regions near lateral boundaries are not justified at the present time.

Power integrals

The most direct connection that can be made across the scales is that based upon "power integrals" as introduced by Stern (1975) and discussed by Joyce (1980). In a turbulent flow field, any structures in the C field would be dissipated at a rate,

$$\chi_C = 2\kappa_C \left(\left(\overline{\frac{\partial^2 C_{lm}}{\partial x_1^2}} \right)^2 + \overline{\left(\frac{\partial^2 C_{lm}}{\partial x_2^2} \right)^2} + \overline{\left(\frac{\partial^2 C_{lm}}{\partial x_3^2} \right)^2} \right), \tag{11}$$ {chi}

(the derivatives in Eq. (11) are negligible for scales larger than l_m) where the overbar denotes a space and/or time-average. Then in a statistically steady-state ocean, the input of this variance, integrated over the ocean is,

$$\iint_{\text{Surfaces}} CQ_C dA = \iiint_{\text{Vol.}} \chi_C dV, \tag{12}$$ {diss1}

and the integrals are taken over the ocean boundary area, particularly the surface, but including all generation boundaries, and the volume respectively, so that the generation-rate balances the dissipation rate. Q_C is a measure of the transfer of C to the ocean volume from the atmosphere and other boundaries under the assumption, in the steady-state, that

$$\iint Q_C dA = 0. \tag{13}$$

If Q_C and C are covarying, the resulting variance generated must be dissipated at the molecular scale, all physics of scale transformations being integrated out in Eq. (12). Generated variances on the left must be consumed in the term on the right at the molecular level, otherwise, the spatial variance of C would grow without bound. (See Schanze and Schmitt (2013) for the complications introduced by various nonlinearities.) The special case of $C = T$ corresponds to entropy conservation. Much of the dissipation, like the generation, occurs within surface the mixed-layer, but significant structures remain in the oceanic interior that must be removed at the molecular scale.

These arguments can be generalized to certain types of oceanic regional subvolumes. Using Eqs. (11), (12) to solve for κ_C gives values (for temperature and salinity) roughly consistent with those obtained from completely different methods (and with very different error bars). All observations do, however, remain highly uncertain; see Schneider and Bhatt (2000).

Consider now the analogue of Eq. (11) for the velocity field, defined as $\mathbf{v} = (u_1, u_2, u_3) = (u, v, w)$, and the latter being the Cartesian special case, but the first form permitting the use of indices. The dissipation of kinetic energy in the ocean, ultimately at similar molecular scales, is usually written as

$$\varepsilon = \frac{\nu}{2} \sum_{i,j=1}^{3} \sum_{i',j'=1}^{3} \left(\frac{\partial u_i}{\partial x_j} \frac{\partial u_{i'}}{\partial x'_j} \right) \tag{14}$$

ν is the ordinary molecular kinematic viscosity and which would again be dominated by the l_m spatial scale. If the turbulence lies mainly in isotropic motions at the smallest scales, the above simplifies to,

$$\varepsilon = \frac{15}{2} \nu \sum_{ij} \left(\frac{\partial u_i}{\partial x_j} \right)^2, \tag{15}$$

for any i, j. The connection between ε, χ, is exploited in the measurements described below. The "Kolmogoroff length-scale", $l_K = \left(\nu^3/\varepsilon\right)^{1/4}$ is a measure of the smallest turbulence scale

present in the fluid, and complete measurement of dissipation in the ocean would have to reach to distances of order 1 cm and less.

Large-scale forces acting on the ocean (e.g., winds and tides with time-scales ranging from the mean to short-lived squalls) are communicated to the ocean through processes which generate motions on all of the observed flow-scales. The wind and other generation processes can also destroy previously-produced structures, and thus Q must be interpreted as the *net* production in the boundary regions.

Vertical Mixing

Quasi-Analytic Model Estimates

The most influential attempt at estimating an element of $\mathbf{K}$ was for the vertical (diapycnal) component K_{33}, with the advection-diffusion Eq. (9) written as the special case of a one-dimensional steady-state balance,

$$w\frac{\partial C}{\partial x_3} - \frac{\partial}{\partial x_3}\left(K_{33}\left(x_3\right)\frac{\partial C}{\partial x_3}\right) = 0. \tag{16}$$ {abyssal1}

For constant w, and K_{33}, the solution is a simple constant plus exponential,

$$C = C_0 + C_1 \exp\left(wx_3/K_{33}\right). \tag{17}$$ {abyssal2}

In widely influential paper, Munk (1966), noting the generally horizontal nature of isopycnals in the open Pacific Ocean, inferred w/K_{33} from fitting the Eq. (17) profiles of temperature and salinity below 1000 meters. Earlier, Wyrtki (1962) used passive oxygen and nutrient distributions which, however, involve interior sources and sinks having significant uncertainties. By also employing radiocarbon as a tracer with a decay term on the right hand side, Munk was able to separately distinguish $w \approx 10^{-7} m/s, K_{33} \approx 10^{-4}\mathrm{m}^2/\mathrm{s}$, assuming the parameters applied identically to temperature, salinity (or linearized density), and radiocarbon—as would be true in conventional turbulence. In the then convention of centimeter-gram-second (CGS) units, the result was the memorable ("canonical") value K_{33} =1 cm^2/s.

Earlier "thermocline models" (e.g., Stommel and Webster, 1962; Welander, 1971) implicitly included Eq. (16) as a special case. These remarkable nonlinear solutions showed however, that "perfect fluid" (adiabatic, $\mathbf{K} = \mathbf{0}$) models gave a gross structure in the thermocline (roughly 300-1000m depth) similar to the observed temperatures and salinities and visually indistinguishable from those with significant vertical mixing. Munk's "abyssal recipe" was widely mis-applied in that upper ocean region, where he had made no claims about K_{33}, and there arose a sense that a contradiction existed between the one-dimensional balance and a possible near-adiabatic

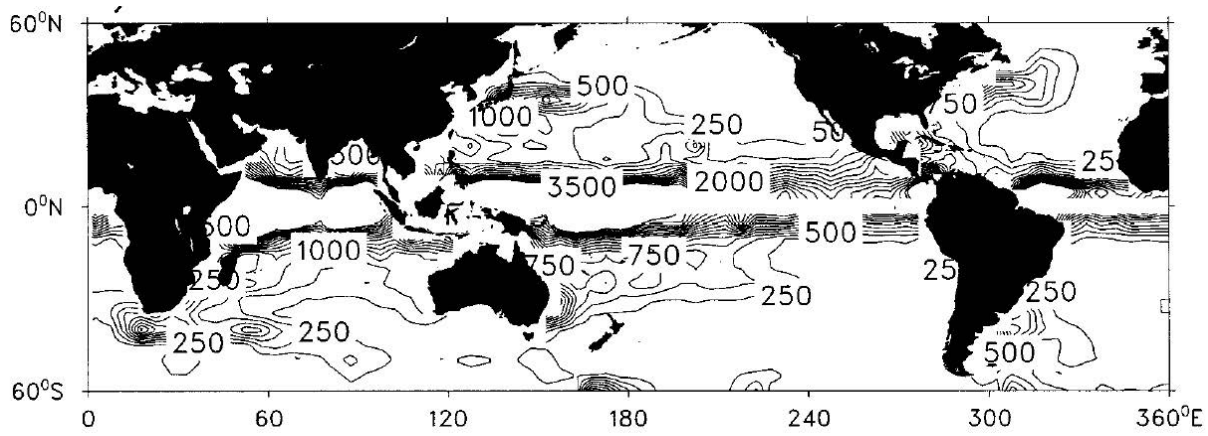

Figure 4: Estimated values of $K_{11} = K_{22}$ (m^2/s, Stammer, 1998) from altimetric variability. The equatorial region is omitted because of the breakdown of geostrophic balance there.

{stammer_jpo19

upper ocean. The seeming-paradox was only resolved with the development of direct field measurements, taken up below.

Lateral Mixing

Lateral analogues in the horizontal dimension, for determining $K_{11,22}$, using large-scale observed horizontal gradients have a long history. An example is discussed by Needler and Heath (1975) and Hogg (1987) who, using the conspicuous feature of the Mediterranean Salt Tongue, did a simultaneous least-squares fit for both vertical and horizontal values. The latter found $K_{11} = K_{22} \approx 500$ m^2/s, $K_{33} \approx 5 \times 10^{-5} m^2/s$.

In more recent years, with the availability of near-global altimetric measurements of surface geostrophic flows, a number of attempts have been made to estimate $K_{11,22}$ directly from the eddy variability. Starting with Holloway (1986) and Stammer (1997), estimates range from about 250 m^2/s in the quiescent eastern parts of the ocean to nearly 3500 m^2/s in the eddy-intensified areas of the low-latitude western-boundary regions (Fig. 4). Numerous regional estimates have been published subsequently, with a particular emphasis in recent years on the eddy-rich Southern Ocean.

The lateral terms K_{1*}, K_{2*} where the $*$ denotes any of the 3-indices $1, 2, 3$ are commonly identified primarily with the powerful kinetic energy of the balanced eddies, and within a modelling context have been the subject of a wide variety of proposals and tests. Recall, however, that the quasi-time average flow field has numerous spatial scales far smaller than the largest scale defining the general circulation. Boundary currents such as the Kuroshio and Gulf Stream on the west, the Equatorial Undercurrents and their associated shear fields, as well as flows on

eastern boundaries, are all capable of stretching and greatly extending the mixing volumes of tracers. But because the modelling community has focussed on parameterizing the mesoscale elements of $\mathbf{K}$, comparatively little is known about the mixing processes in strongly sheared boundary currents. More generally, the presence of strong horizontal flows (boundary currents, the circumpolar current) implies that the interaction of the balanced eddy field with those motions cannot be ignored. Note in particular (Ferrari and Nikurashin, 2010; Klocker et al., 2012) that the horizontal elements of $\mathbf{K}$ are apparently suppressed near-surface at the core of the Antarctic Circumpolar Current, and presumably in other strongly sheared currents. In the same currents, excess mixing can occur at depth in the "critical levels" where the phase velocity of the eddy disturbance coincides with the velocity of the mean shear (Abernathey et al., 2010).

Lateral mixing has also been studied via the separation (dispersion) of clusters of pseudo-Lagrangian floats (Lacasce, 2008) as well as from data arising from the purposeful dye experiments. As with K_{33}, realistic numerical models of the ocean must accommodate a complex and highly detailed spatial structure in the lateral components of the mixing tensor. Whether the temporal variations, owing to variations in time of energy inputs to the ocean are significant and if so, on what time-scales, remains largely unknown.

Vertical Mixing: Direct Field Measurements

The discovery of what is now called "microstructure" on scales of centimeters in vertical profiles of temperature and salinity in the middle 1960s, through the newly available profiling instruments (see Baker, 1981) led to the realization that the observed structures were an indicator of the direct actions of molecular processes in the oceanic circulation. ("Fine structure" is commonly defined as appearing on the larger, meter, scales.)

Profiling instruments that measure the turbulent velocities have led to numerous direct estimates of diapycnal or vertical mixing rates. Osborn (1980) proposed that the relationship between the turbulent mixing coefficient and the measured dissipation could be calculated as,

$$K_{33} = \frac{\Gamma \langle \varepsilon \rangle}{N^2}, \tag{18}$$ {osborn}

where ε is defined in Eq. (12), brackets indicate an average, and $N = \sqrt{-(g/\rho)\,\partial\rho/\partial x_3}$ is the buoyancy frequency. Γ is the so-called mixing efficiency which is widely taken to be approximately 0.2, but a growing body of evidence suggests that it can vary condiderably (Inoue and Smyth, 2009; Lozovatsky and Fernando, 2013). Its physical interpretation is as the fraction of the turbulent energy that goes into mixing, noting that it must vanish in an unstratified fluid. Variations in Γ by factors of two or three are not usually the limiting uncertainty in calculations involving Eq. (18), but eventually it must not be treated as a universal constant.

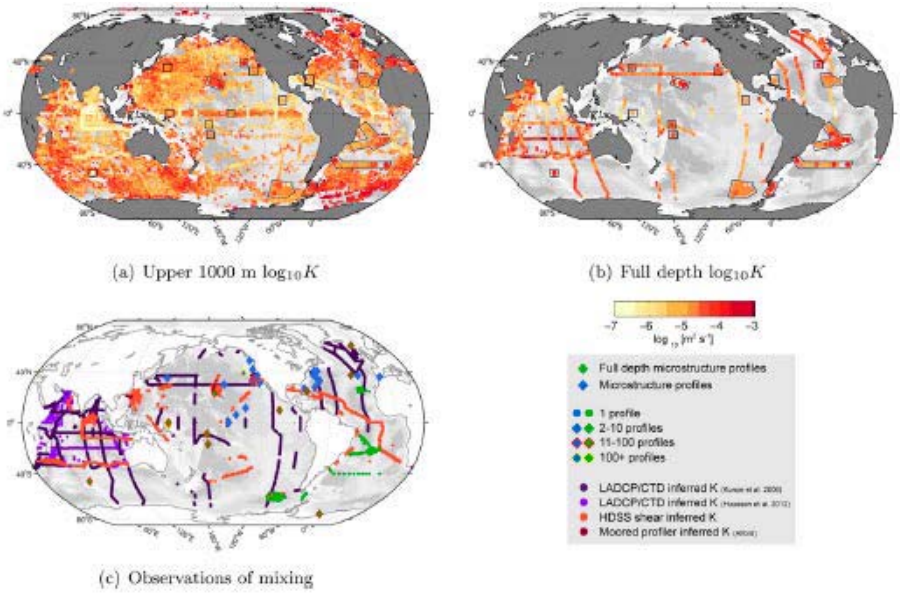

Figure 5: From Waterhouse et al. (2014) showing estimated values of K_{33} over the top 1000m (a) and averaged over the full depth (b) with many fewer measurements). (c) Shows the different types of measurements used for calculations. LADCP is lowered doppler current profiler; CTD is conductivity, temperature, depth; HDSS is hydrographic doppler sonar system. {waterhouse_et

An alternative measure (Osborn and Cox, 1972) is based directly on measurements of χ_T in the form,

$$K_{33} = \frac{\langle \chi_T \rangle}{2\left(\frac{\partial \bar{T}}{\partial x_3}\right)}. \tag{19}$$ {osborn-cox}

The two methods should produce identical results where only temperature controls the stratification. Merrifield et al. (2016) discuss the differences when salinity becomes a factor. A major issue with Eqs. (18, 19) is that few instruments are capable of measuring the full spectrum of motions down to the Kolmogoroff scale, l_K in ε, or the even smaller equivalent Batchelor-scale, $l_B = \sqrt{\kappa^2 \nu/\varepsilon}$, for temperature. Thus the unresolved contributions to ε or χ_T must come from extrapolation. Some of these extrapolation formulae are quite complex. Waterhouse et al. (2014) have compiled a global calculation of K_{33} from a very large variety of velocity profile measurements and extrapolations, taken over the years, and a fixed value of Γ in Eq. (18), and are shown in Fig. 5). Upper ocean values are generally of order $10^{-5}\mathrm{m}^2/s$, with higher values in the very high latitudes. Values at depth derive from very sparse sampling and tend to be higher over topographic features, e.g., the Mid-Atlantic Ridge in the South Atlantic Ocean.

Fig. 6 shows an approximate breakdown of their results by topographic roughness type. Abyssal plain values are nearly uniform with depth, while those over rough topography, and

particularly over the mid-ocean ridges show a pronounced increase towards the bottom. Any calculation today of global mean abyssal values from these measurements would be highly uncertain.

Vertical Mixing: Volumetric Inverse Methods

Profiling instruments produce measurements at single points, and even in Fig. 5 they remain sparse in both space and time, conspicuously so at depth.. A different approach to determination of K_{33} comes from integrating geostrophic flows over large volumes lying between isopycnals—and including boundary effects—in geostrophic box models. A closely related approach is through the $\beta-$spiral (e.g., Olbers et al., 1985; Fukumori, 1991).

A particularly simple example is that of Hogg et al. (1982) who found that the deep Brazil Basin had to have a value of K_{33} of about $10^{-4}\mathrm{m}^2/\mathrm{s}$, not inconsistent with the abyssal recipes canonical value. Later profiling measurements—Toole et al. (1997)—show the volumetric average there as being dominated by much higher values over and near the Mid-Atlantic Ridge and lower values over the abyssal plain. Various box inversions (e.g., Ganachaud 2003, Lumpkin and Speer, 2007, Macdonald et al., 2009) have produced basin-scale estimates ranging from about 2×10^{-5} to 3×10^{-4} , depending upon the location and depth as well as assumptions about detailed rates of flow. These results combine the effects of interior and lateral boundary/-topography mixing rates. All have significant stated uncertainties. Many places (Ganachaud, 2003) show an increasing K_{zz} towards the bottom. A number of studies (e.g., Sloyan and Rintoul, 2000) have estimated the net diapycnal flux.

Of particular interest have been the experiments with purposeful dye releases in the open ocean (e.g., Watson et al., 2013) which tend to give higher mixing rates than have been inferred from local profiling measurements—again probably best interpreted as an indication of higher intensity mixing near boundary topographies of various sorts (Mashayek et al., 2016).

Boundary Mixing

Munk (1966) had noted in passing that oceanic mixing could be greatly enhanced at the sidewall boundaries of the ocean. Stimulated by the intense motions generated on sloping boundaries by the internal wave field, Phillips (1970) and Wunsch (1970) examined the flows at the boundaries where no flux into the solid is permitted. Later examinations include that of Dell and Pratt (2015). No simple separation into vertical and horizontal effects is possible in those regions.

The peculiar properties of internal waves on sloping boundaries, leading to intense breaking, and boundary layer instabilities (Ivey et al., 2000) seen in the laboratory led to fine and

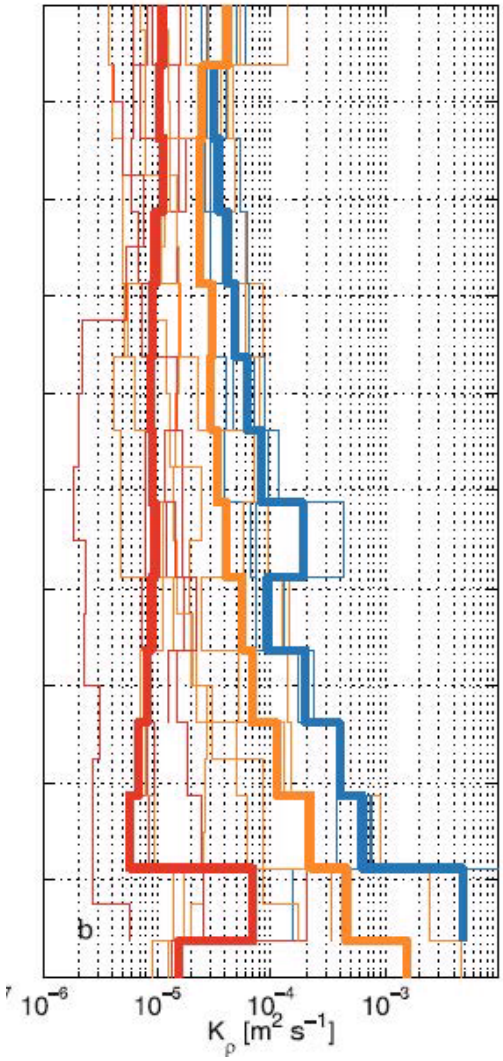

Figure 6: Diffusivity K_{33} for density as estimated by Waterhouse et al. (2013). Thick red curve is the average profile over smooth topography, thick orange curve is from rough topography and thick blue from ocean ridges. General increase towards the bottom is evident, particularly over the latter two regions. Thin lines show the scatter of each type.

{waterhouse_et

microstructure measurements, first near islands and seamounts (Wunsch, 1972; Hogg et al., 1978; Eriksen, 1998) and to work on continental margins (e.g., Lamb, 2014). Direct experiments with injected artificial dyes (e.g., Ledwell et al., 2016) have confirmed that excess mixing does occur through various processes at continental boundaries. The collection of papers found in Imberger (1998) provides a useful overview. Oceanic canyons, both on continental margins and in the mid-ocean ridges also show strongly increased mixing, likely associated with internal wave instabilities of various kinds (see Kunze et al., 2002, Thurnherr et al., 2005). Armi (1978) calculated the effect of ambient flow and associated turbulence on sloping topography, but which gave rise to debate (see Garrett et al., 1993) concerning the influence of that mixing on the interior stratification. At the present time, it does appear that sloping boundary turbulence and consequent mixing are dominated by the complex motions and breaking from the internal wave field, including the internal tide. Whether the maximum effective mixing rates occur in the boundary layers, or in the interior region above the boundary layer is not so clear. Garrett et al. (1993) have argued that boundary layers tend to mix already mixed fluid and so are relatively ineffective compared to the enhanced breaking of internal waves just above the bottom.

A sweeping generalization would be that the Munk canonical value for a vertical mixing coefficient of about $10^{-4}\mathrm{m}^2/\mathrm{s}$ applies primarily to the deep ocean (somewhere deeper than the 1 km depth he focussed on), as an average of much smaller interior values (below $10^{-5}\mathrm{m}^2/\mathrm{s}$) and much higher values over topographic features, with generally increasing values as the topography (on many scales) is approached from above (See Toole et al., 1994; Munk and Wunsch, 1998). Regions with very small values of inferred K_{33} imply correspondingly very small values of the vertical velocity, w, in those places (see the next section), with major consequences for the behavior of the large-scale circulation. Furthermore, the strong increase of K_{33} toward the oceanic floor, away from the abyssal plains, gives rise to somewhat unexpected overall behavior through terms such as $\partial K_{33}/\partial x_3$ (Ferrari et al., 2016) which act in the advection-diffusion equation as an equivalent abyssal vertical velocity.

Boundary mixing is included in the inverse box model inversions where hydrographic lines terminate in topographic features, but not in most of the profiling measurements. Comparisons of volume averages from box models with point measurements from profilers are thus difficult.

In the region above 1-2 km in the water column, the dominant values of $K_{33} \leq 10^{-5}\mathrm{m}^2/\mathrm{s}$ are consistent with the thermocline theories treating the motion as nearly non-diffusive. Much recent attention has thus focussed on the outcrop regions of the isopycnals/neutral surfaces in the Southern Ocean, where direct wind mixing, within the surface mixed-layer/Ekman layer, likely provides most of the transformation of water properties required by the observed upper-ocean circulation.

Exchanges between the oceanic interior and fluid in the boundary layers of the sidewalls (recalling that their slope is usually less than 3°) requires special treatment in its own right (e.g., Phillips et al., 1986; Garrett et al., 2013; Dell and Pratt, 2015) and may (Ferrari et al., 2016) control the interior circulation. Attention in the next several years is likely to further focus on the interaction of ocean flows on all scales with boundary features of all types.

Consequences of Spatial Variations

The existence of regions of strongly enhanced values of K_{ij}, particularly the orders of magnitude found in K_{33}, greatly complicates quantitative calculations of effective rates of mixing. Not only does the spatial variation have important consequences for the ocean circulation on the largest, L, scale, but the residence time of fluid within those "hotspots" is a function of the large-scale circulation itself (Mashayek et al., 2016).

The simplest dependence on the spatial structure can be seen from the important dynamical relationship in a mainly geostrophically balanced ocean in the linear vorticity equation,

$$\beta v = f \frac{\partial w}{\partial z} \tag{20}$$

where v is the meridional velocity, and β is the local meridional derivative of the Coriolis parameter, f. To have a meridional flow requires a finite w (the conventional Eulerian vertical component) with finite derivative. On the other hand, in regions of nearly horizontal isopycnals, Eq. (16) shows that the existence of w depends directly upon the existence of a finite K_{33}. Weak values of vertical mixing, in the absence of steeply sloping isopycnals, imply weak or non-existent w, and hence a strong limit on any meridional flow.

In the "abyssal recipe" of Eq. (16), a steady-state e.g., of temperature, $C = T$ is maintained with a constant K_{33} as a balance between the downward diffusion of heat from the high temperatures near the surface, and the upward advection cold water from below. But if the assumption of a vertically constant K_{33} is abandoned, the situation can be very different. Suppose by way of example that the abyssal ocean has a constant temperature gradient, $\partial T/\partial x_3 = T_0'$, then Eq. (16) becomes

$$w = \frac{\partial K_{33}}{\partial x_3} \tag{21}$$ {wfromk}

and if, as now seems clear (Fig. 5), K_{33} is often largest near the ocean bottom, $w < 0$ and the balance is now that of the *downward advection* of temperature against the *upward diffusion* of cold water.[2] An implication is the reversal of the standard picture of an upward movement

[2] The argument that true mixing can only increase the potential energy applies only to the net effects over the entire volume.

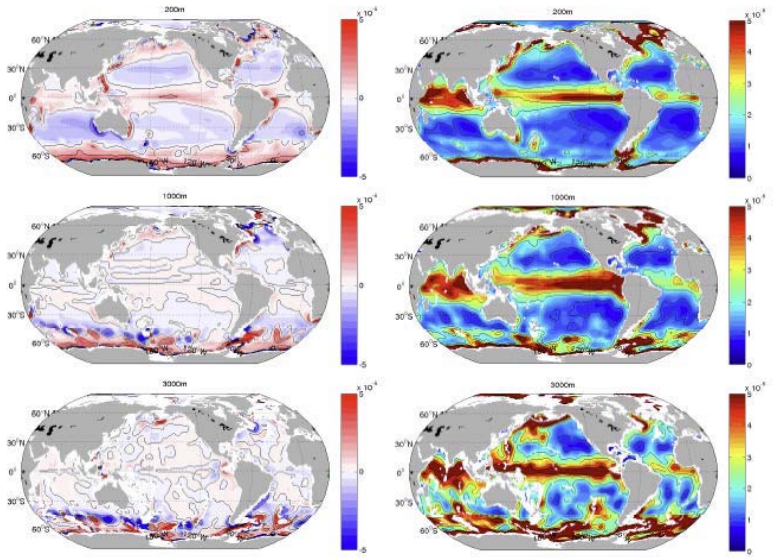

Figure 7: A 20-year average estimated Eulerian w from a highly constrained general circulation model (a "state-estimate"; see Forget et al., 2015). Values at three depths are shown in the left-column, temporal standard deviations in the right-column. 200m values are dominated by the Ekman pumping of the mean wind, while the deepest values at 3000m are topographically controlled. Intermediate depth displays a combination of both fields. (X. Liang, 2015, personal communication). The complex reversals show that some universally valid description about the nature of vertical ocean fluxes is likely not possible. {liang_vertica

of water balancing high latitude convection of dense, deep water to the abyss. The product of the density profile with that of K_{33} determines the sign of w. A more general derivation of this result, with a discussion of the potential consequences for the general circulation, is given by Ferrari et al. (2016).

The implied values of w from Eq. (21) will have a lateral variability that is as large or larger than that seen in K_{33} itself. Fig. 7 displays a 20-year average and its standard deviation obtained from a state estimate (an ocean general circulation model fit to the data by constrained least-squares). Among other implications is that the Eulerian w field in the ocean is expected to be extremely noisy; Fig. 7 displays an estimate of w at three depths. The spatial structures, particularly at depth, are complex even with 20-years of averaging. Liang et al. (2016) showed equivalent maps of the net time-averaged $w^* = w + w_{eddy}$ arising both from the Eulerian and eddy-induced values. No global generalization, even about just the open ocean values of w or w^*, is likely to be accurate. No reconciliation yet exists of the inferences from the Munk (1966) model, and those deriving from the intense spatial variability.

Upper Ocean/Mixed Layer

The surface layers of the ocean, in direct contact with the atmosphere have a specialized mixing literature of their own (D'Asaro, 2014). Surface outcrop areas of isopycnals visible in Fig. 3 and in other oceans are of particular importance. Exchanges between the mixed layer and the ocean below have focussed on the influence of the sub-mesoscale, particularly as it influences the nutrient transfers, and hence the biology (e.g., Mahadevan, 2016).

Vertical Mixing: The Energy Problem

In the underlying Navier-Stokes equations such as (1), κ_C derives from the vibrational and other motions of molecules powered by the internal energy of the fluid. Consider that an isolated thermally stratified fluid will, after sufficiently long time, become uniform in temperature, with a consequent increase in its potential energy—the center of mass having been moved upward and with the internal energy correspondingly reduced. In numerical models, where the coefficients such as $\mathbf{K}$ are commonly introduced as ad hoc parameters representing the action of eddies on the larger scale L, no explicit source of energy has been specified. Beginning in the late 1990s, attention began to turn toward understanding of the complete oceanic energy budget including, specifically, the source of energy powering the stirring carrying the mixing the final step toward the molecular scale.

Energy suppliers for the turbulent stirring and mixing are identical to those powering the overall general circulation and thus a clean separation of sources is not possible. Such overall power sources include: (1) the wind; (2) tides; (3) precipitation and evaporation; (4) heat exchange with the atmosphere; (5) atmospheric pressure changes. Attaching numbers with useful accuracy to these various processes has proved challenging, and the reader is referred for more detail to the article on ocean energetics. A summary would be that (3) and (5) are minor contributors, (1) and (2) are very important, and that evaluating (4) has proven problematic—as it appears to depend strongly on the flows established by (1) as well. Input of energy from the wind is thought to take place primarily on the largest scales, and on the scale of oceanic inertial motions (near the Coriolis frequency, f). Much of the energy input appears first as an increase in oceanic potential energy, prior to its release into kinetic energy by a variety of pathways. Winds are believed to be the major power source for the balanced eddies via baroclinic instabilities, but then can act to destroy them. Tidal input of energy is believed to occur primarily through the conversion at topography of the ordinary surface tides into internal tides on scales far smaller than L.

Understanding the energetics of mixing then depends upon determination of the pathways

by which the energy inputs carry energy down to the point where molecular processes can begin to work efficiently. These pathways and their importance and locales remain poorly quantified. Attention has focussed on internal waves—both interior breaking (see e.g., Munk, 1981; Thorpe, 2010), and the very intense motions they induce on and over slopes of all kinds.

Most of the kinetic energy of the ocean circulation lies in the balanced eddies and they are an obvious source for conversion into smaller scales. As compared to the internal wave field, their vertical and horizontal scales tend to be larger, but in topographic interactions they are capable of generating a large variety of much smaller scales including internal waves and boundary layers. The lifetime of the eddy field has been variously estimated as roughly 6 months (Ferrari and Wunsch, 2009), but where and how the corresponding dissipation occurs is not fully quantified (Zhai et al., 2010; Clément et al., 2016). The direct coupling between geostrophically balanced motions and internal waves is weak (Vanneste, 2013). Also a strong tendency exists in rotationally dominated turbulence to drive energy "upscale", that is to larger, rather than smaller spatial scales (e.g., Vallis, 2006). But turbulent bottom friction, topographic interactions, flow separation at bottom features, all remain viable dissipation candidates.

General Circulation Models (GCMs)

Oceanic kinetic energy (what moves tracers around) is dominated by the balanced eddies. As modelling power has grown, the greatest efforts have been directed at the detailed numerical representation of the balanced eddies in models. In particular, many global models fail to resolve the eddy field, and the numerical parameterization of the effects of balanced eddies has generated a voluminous literature (see the collection of papers in Hecht and Hasumi, 2007). In numerical models the mixing tensor (Eq. 10) is generally formulated in isopycnal coordinates, reflecting the anisotropy of diapycnal and isopycnal mixing. In so-called $z-$coordinate models the resulting tensor is then transformed approximately back to geodetic coordinates. The re-transformation is not required for models written in isopycnal coordinates.

Because lateral motions are much more intense than vertical ones, numerical difficulties arise in preventing artificial vertical diffusivities arising from the horizontal motions, distinguishing between those fields (temperature and salinity) which determine the isopycnals, and the passive tracers that make no such contribution. This complex subject is covered in the textbooks by Haidvogel and Beckmann (1999); Griffies (2004), Vallis (2006), Olbers et al. (2012).

The largest literature focuses on the best numerical representation of $\mathbf{K}$—in all three-dimensions—and its equivalents (the problem of "sub-grid scale parameterization"). In the process, the distinction between stirring and mixing has largely been lost, with the molecular scales assumed to take care of themselves—between the actions of $\mathbf{K}$, and with the inescapable

numerical dissipation becoming a surrogate for the true molecular mixing. Much (not all) of the eddy effect is represented in terms of an equivalent lateral velocity (sometimes called the bolus velocity), and is calculated from the anti-symmetric components of tensor $\mathbf{K}$ (see especially Flierl and McGillicudy, 2002, Section 7; the "skew-flux"), and is related closely to the transformed Eulerian mean (TEM). A common numerical method relies upon extensions and modifications of the proposal of Gent and McWilliams (1990). Because the method, and most of its variants, is focussed on baroclinic instability processes, it removes potential energy from the fluid by flattening isopycnals, rather than increasing it as in mixing. It is thus a scheme for spreading, and not mixing. An explicit dissipation picture for the energy released is lacking.

Many of the isopycnals in the upper 1000m of the ocean—above the domain of Munk's "abyssal recipes"—outcrop at the sea surface in the Southern Ocean (Fig. 3). There the intense turbulence existing in the surface boundary layer, derived directly from the locally powerful wind field, can provide an easy route for mixing the fluid across these density surfaces. (see e.g., the modelling study of von Storch et al., 2007). In the abyss, where the isopycnals do not outcrop to the surface, direct wind-forcing does not act and diapycnal mixing is dependent upon the wave breaking mechanisms.

In a hypothetical ocean model that was capable of directly resolving the centimeter and smaller scales, l, important in $\kappa_C \nabla^2 C$, no parameterizations would be required. Taking the requisite length arbitrarily as 1 mm, vertically and horizontally, a global model would require of order 10^{27} grid points or Fourier components, and thus the need for statistical mechanics and parameterizations will exist indefinitely. Global models in which the balanced eddy field is adequately resolved are on the horizon, but the mixing scales, l_m, remain far beyond direct reach.

Summary Discussion

The remarkable spatial variations now known to exist in ocean mixing processes have many implications for understanding and potential prediction of the ocean circulation and all of its climate consequences. With the coupling amongst motions at all time and space scales, discussion of mixing can hardly be done without a long excursion into all ocean flows and energetics. Spatial variations in effective mixing have powerful implications for the general circulation itself (defined as a time average over several decades) implying a very different picture than was accepted until quite recently.

In seeking gross generalizations, it appears that the tide—directly generating internal waves—and the wind generated instabilities and inertial motions, produce the turbulence that mixes the ocean. Roughly speaking, the equivalent vertical or diapycnal or dianeutral mixing coefficients

range from comparatively low average values in the upper 1000m of about $10^{-5}\mathrm{m}^2/\mathrm{s}$, to an order of magnitude larger below that depth. Very much higher values appear in the surface mixed layer with distinct physics. Values increase in the abyss, over certain types of topographic features, by two or more additional orders of magnitude. The implications are that much of the upper ocean can be treated as a near-perfect fluid, with the necessary mixing occurring at the sea surface at high latitudes. In contrast, the very intense mixing over topographic features implies that vertical exchanges and hence the meridional oceanic motions are confined to very special regions, including lateral boundaries of all types. A general increase in diapycnal mixing toward the sea floor in the open ocean implies a net downward flux of temperature generally, with part of the upwards return flow being a lateral boundary phenomenon—and which represents a radical change in understanding of the deep circulation.

Determination of the influence of the ocean on future climate change requires quantitative prediction of the ways in which energy exchanges with the atmosphere will shift, and in turn how those translate into modifications of the general circulation, its storage and transfers of heat, freshwater, carbon, oxygen, etc. The gross ocean stratification will also change, along with the mixing energetics and rates, as well as will the meteorological interactions. *A priori* calculation of the overall stratification and resulting movement of climate properties in the ocean past, present, and future remains a major challenge.

Acknowledgement. I am grateful to R. Ferrari and C. Garrett for numerous comments and corrections and to the ECCO Consortium for support.

References

Abernathey, R., Marshall, J., Mazloff, M., & Shuckburgh, E. (2010). Critical layer enhancement of mesoscale eddy stirring in the Southern Ocean. Journal of Physical Oceanography, 40, 170-184.

Armi, L. (1978). Some evidence for boundary mixing in the deep ocean. Journal of Geophysical Research-Oceans and Atmospheres, 83(NC4), 1971-1979. doi: 10.1029/JC083iC04p01971

Baker, D. J. (1981). Ocean instruments and experimental design. In B. A. Warren & C. Wunsch (Eds.), Evolution of Physical Oceanography. Scientific Surveys in Honor of Henry Stommel. Cambridge MA: The MIT Press.

Batchelor, G. K. (1953). The Theory of Homogeneous Turbulence: Cambridge Un. Press.

Canuto, V. M., Cheng, Y., & Howard, A. M. (2007). Non-local ocean mixing model and a new plume model for deep convection. Ocean Modelling, 16, 28-46. doi: http://dx.doi.org/10.1016/j.ocemod.2006.07.0

Clément, L., Frajka-Williams, E., Sheen, K. L., Brearley, J. A., & Garabato, A. C. N. (2016). Generation of internal waves by eddies impinging on the western boundary of the North Atlantic. Journal of Physical Oceanography, 46(4), 1067-1079. doi:10.1175/JPO-D-14-0241.1

D'Asaro, E. A. (2014). Turbulence in the upper-ocean mixed layer. Annual Review of Marine Science, 6(1), 101-115. doi:10.1146/annurev-marine-010213-135138

Davis, R. E. (1994). Diapycnal mixing in the ocean: equations for large-scale budgets. Journal of Physical Oceanography, 24(4), 777-800. doi: 10.1175/1520-0485

Defant, A. (1961). Physical Oceanography, Vol. 1. New York: Pergamon.

Dell, R. W., & Pratt, L. J. (2015). Diffusive boundary layers over varying topography. Journal of Fluid Mechanics, 769, 635-653.

Eckart, C. (1948). An analysis of the stirring and mixing processes in incompressible fluids. Journal of Marine Research, 7(3), 265-275.

Eriksen, C. C. (1998). Internal wave reflection and mixing at Fieberling Guyot. J. Geophys. Res., 103, 2977-2994.

Ferrari, R., Mashayek, A., McDougall, T. J., Nikurashin, M., & Campin, J.-M. (2016). Turning ocean mixing upside down. Journal of Physical Oceanography, 46, 2239-2261.

Ferrari, R., & Nikurashin, M. (2010). Suppression of Eddy Diffusivity across Jets in the Southern Ocean. Journal of Physical Oceanography, 40(7), 1501-1519. Ferrari, R., & Wunsch, C. (2009). Ocean circulation kinetic energy: reservoirs, sources, and sinks. Annual Review of Fluid Mechanics, 41, 253-282. doi: DOI 10.1146/annurev.fluid.40.111406.102139

Flierl, G., & McGillicuddy, D. J. (2002). Mesoscale and submesoscale physical-biological interactions. In A. R. Robinson, J. J. McCarthy & B. J. Rothschild (Eds.), The Sea, Vol. 12,113-185.

New York: John Wiley & Sons.
Forget, G., Campin, J.-M., Heimbach, P., Hill, C., Ponte, R., & Wunsch, C. (2015). ECCO version 4: an integrated framework for non-linear inverse modeling and global ocean state estimation. Geosci. Model Dev., 8, 3071?3104.
Fukumori, I. (1991). Circulation about the Mediteranean Tongue: An analysis of an EOF-based ocean. Prog. in Oceanog., 27, 197-224.
Garrett, C., Maccready, P., & Rhines, P. (1993). Boundary mixing and arrested Ekman layers—rotating stratified flow near a sloping boundary Annual Review of Fluid Mechanics, 25, 291-323. doi: 10.1146/annurev.fl.25.010193.001451
Griffies, S. M. (2004). Fundamentals of Ocean Climate Models: Princeton U. Press.
Haidvogel, D. B., & Beckmann, A. (1999). Numerical Ocean Circulation Modeling: Imperial College Press, River Edge, NJ.
Hecht, M. W., & Hasumi, H., (Eds.). (2008). Ocean Modeling in an Eddying Regime. Washington, D.C.: American Geophysical Union.
Helland-Hansen, B., & Nansen, F. (1909). The Norwegian Sea: Its Physical Oceanography Based Upon the Norwegian Researches 1900-1904. Report on Norwegian Fishery and Marine Investigations 2. Kristiania: Det Mallingske bogtrykkeri.
Hogg, N. G. (1987). A least-squares fit of the advective-diffusive equations in Levitus Atlas data. Journal of Marine Research, 45, 347-375.
Hogg, N. G., Katz, E. J., & Sanford, T. B. (1978). Eddies, islands, and mixing. Journal of Geophysical Research-Oceans and Atmospheres, 83(NC6), 2921-2938. doi: 10.1029/JC083iC06p02921
Holloway, G. (1986). Estimation of oceanic eddy transports from satellite altimetry. Nature, 323, 243-244.
Huang, R. X. (1999). Mixing and energetics of the oceanic thermohaline circulation.Journal of Physical Oceanography, 29, 272-746.
Imberger, J. E. (1998). Physical Processes in Lakes and Oceans. Washington, DC: American Geophysical Union.
Inoue, R., & Smyth, W. D. (2009). Efficiency of Mixing Forced by Unsteady Shear Flow. Journal of Physical Oceanography, 39(5), 1150-1166. doi: 10.1175/2008jpo3927.1
Ivey, G. N., & Winters, K. B., De Silva, I. P. D. (2000). Turbulent mixing in a sloping benthic boundary layer energized by internal waves. Journal of Fluid Mechanics, 418, 59-76.
Klocker, A., Ferrari, R., & LaCasce, J. H. (2012). Estimating suppression of eddy mixing by mean flows. Journal of Physical Oceanography, 42(9), 1566-1576. doi: 10.1175/jpo-d-11-0205.1
Kunze, E., Rosenfeld, L. K., Carter, G. S., & Gregg, M. C. (2002). Internal waves in Monterey Submarine Canyon. Journal of Physical Oceanography, 32(6), 1890-1913. doi:10.1175/1520-

0485(2002)032<1890:IWIMSC>2.0.CO;2
LaCasce, J. H. (2008). Statistics from Lagrangian observations. Progress in Oceanography, 77(1), 1-29.
Lamb, K. G. (2014). Internal wave breaking and dissipation mechanisms on the continental slope/shelf. In S. H. Davis & P. Moin (Eds.), Annual Review of Fluid Mechanics, Vol 46, 231-254.
Ledwell, J. R., He, R., Xue, Z., DiMarco, S. F., Spencer, L., & Chapman, P. (2016). Dispersion of a tracer in the deep Gulf of Mexico. Journal of Geophysical Research: Oceans, 2169-9291.
Liang, X., Wunsch, C., Heimbach, P., & Forget, G. (2016). Vertical redistribution of oceanic heat content. Journal of Climate, 28, 3821-3833.
Lozovatsky, I. D., & Fernando, H. J. S. (2013). Mixing efficiency in natural flows. Philosophical Transactions of the Royal Society A: Mathematical, Physical and Engineering Sciences, 371(1982). doi: 10.1098/rsta.2012.0213
Lumpkin, R., & Speer, K. (2007). Global ocean meridional overturning. Journal of Physical Oceanography, 37, 2550-2562. doi: 10.1175/jpo3130.1

Mahadevan, A. (2016). The impact of submesoscale physics on primary productivity of plankton. In C. A. Carlson & S. J. Giovannoni (Eds.), Annual Review of Marine Science, Vol 8, 161-184).
Mashayek, A., Ferrari, R., Merrifield, S., Ledwell, J., St. Laurent, L., & Naveira Garabato, A. (2016). Topographic enhancement of vertical turbulent mixing in the Southern Ocean. Nature Comm., in press.
McDougall, T. J., & Garrett, C. J. R. (1992). Scalar conservation equations in a turbulent ocean. Deep-Sea Research Part A- 39 (11-12A), 1953-1966. doi: 10.1016/0198-0149(92)90007-g
McWilliams, J. C. (2008). The nature and consequences of oceanic eddies. In M. W. Hecht & H. Hasumi (Eds.), Ocean Modeling in an Eddying Regime (Vol. 177, pp. 5-15): AGU Monograph.
Merrifield, S. T., Laurent, L. S., Owens, B., Thurnherr, A. M., & Toole, J. M. (2016). Enhanced diapycnal diffusivity in intrusive regions of the Drake Passage. Journal of Physical Oceanography, 46(4), 1309-1321. doi:10.1175/JPO-D-15-0068.1
Munk, W. (1981). Internal waves and small-scale processes. In B. A. Warren & C. Wunsch (Eds.), in Evolution of Physical Oceanography. Scientific Surveys in Honor of Henry Stommel (pp. 264-291): The MIT Press, Cambridge, Ma (also at http://ocw.mit.edu/ans7870/resources /Wunsch/wunschtext.htm).
Munk, W., & Wunsch, C. (1998). Abyssal recipes II: energetics of tidal and wind mixing. Deep-Sea Res., 45, 1976-2009.

693 Munk, W. H. (1966). Abyssal recipes. Deep-Sea Res., 13, 707-730.
694 Nash, J. D., Kunze, E., Toole, J. M., & Schmitt, R. W. (2004). Internal tide reflection and
695 turbulent Mixing on the continental slope. Journal of Physical Oceanography, 34(5), 1117-1134.
696 doi:10.1175/1520-0485(2004)034<1117:ITRATM>2.0.CO;2
697 Needler, G. T., & Heath, R. A. (1975). Diffusion coefficients calculated from the Mediterranean
698 salt anomaly in the North Atlantic Ocean.
699 Olbers, D., J. M. Wenzel, & Willebrand, J. (1985). The inference of North Atlantic circulation
700 patterns from climatological hydrographic data. Revs. Geophys., 23, 313-356.
701 Olbers, D., Willebrand, J., & Eden, C. (2012). Ocean Dynamics. Berlin ; New York: Springer.
702 Osborn, T. R. (1980). Estimates of the local rate of vertical duffusion from dissipation measure-
703 ments.Journal of Physical Oceanography, 10, 83-89.
704 Osborn, T. R., & Cox, C. S. (1972). Oceanic fine structure. Geophys. Fl. Dyn., 3, 321-345.
705 Ottino, J. M. (1989). The Kinematics of Mixing: Stretching, Chaos, and Transport: Cambridge
706 U. Press, Cambridge.
707 Phillips, O. M. (1970). On flows induced by diffusion in a stably stratified fluid. Deep-Sea Res.,
708 17, 435-443.
709 Phillips, O. M., Shyu, J. H., & Salmun, H. (1986). An experiment on boundary mixing—mean
710 circulation and transport rates. Journal of Fluid Mechanics, 173, 473-489.
711 Radko, T. (2013). Double Diffusive Convection. Cambridge: Cambridge Un. Press.
712 Salmon, R. (1998). Lectures on geophysical fluid dynamics. New York: Oxford University Press.
713 Schanze, J. J., & Schmitt, R. W. (2013). Estimates of cabbeling in the global ocean. Journal of
714 Physical Oceanography, 43(4), 698-705. doi: 10.1175/jpo-d-12-0119.1
715 Schneider, E. K., & Bhatt, U. S. (2000). A dissipation integral with application to ocean diffu-
716 sivities and structure. Journal of Physical Oceanography, 30(6), 1158-1171. doi: 10.1175/1520-
717 0485(2000)030<1158:adiwat>2.0.co;2
718 Sheen, K. L., Brearley, J. A., Garabato, A. C. N., Smeed, D. A., Waterman, S., Ledwell, J. R.,
719 Watson, A. J. (2013). Rates and mechanisms of turbulent dissipation and mixing in the South-
720 ern Ocean: Results from the Diapycnal and Isopycnal Mixing Experiment in the Southern Ocean
721 (DIMES). Journal of Geophysical Research-Oceans, 118(6), 2774-2792. doi: 10.1002/jgrc.20217
722 Sloyan, B. M., & Rintoul, S. R. (2000). Estimates of area-averaged diapycnal fluxes from
723 basin-scale budgets. Journal of Physical Oceanography, 30(9), 2320-2341. doi:10.1175/1520-
724 0485(2000)030<2320:EOAADF>2.0.CO;2
725 Stammer, D. (1997). On eddy characteristics, eddy mixing and mean flow properties.Journal of
726 Physical Oceanography, 28, 727-739.
727 Stern, M. E. (1975). Ocean Circulation Physics: Academic New York.

728 Stommel, H., & Webster, J. (1962). Some properties of thermocline equations in a subtropical
729 gyre. Journal of Marine Research, 20, 42-56..
730 Talley, L. D. (2007). Hydrographic Atlas of the World Ocean Circulation Experiment (WOCE)
731 Volume 2: Pacific Ocean (Eds. M. Sparrow, P. Chapman, and J. Gould): http://www-pord.ucsd.edu/whp.mscatlas
732 Tennekes, J., & Lumley, J. L. (1972). A First Course in Turbulence: The MIT Press.
733 Thorpe, S. A. (2005). The Turbulent Ocean. Cambridge ; New York: Cambridge University
734 Press.
735 Thorpe, S. A. (2007). An Introduction to Ocean Turbulence: Cambridge.
736 Thorpe, S. A. (2010). Breaking internal waves and turbulent dissipation. [Article]. Journal of
737 Marine Research, 68(6), 851-880.
738 Thurnherr, A. M., L. C. St. Laurent, K. G. Speer, J. M. Toole, & Ledwell, J. R. (2005). Mixing
739 associated with sills in a canyon on the Midocean Ridge flank.Journal of Physical Oceanography,
740 35, 1370-1381.
741 Toole, J. M., K. L. Polzin„ & Schmitt, R. W. (1994). Estimates of diapycnal mixing in the
742 abyssal ocean. Science, 264, 1120-1123.
743 Vallis, G. K. (2006). Atmospheric and Oceanic Fluid Dynamics: Fundamentals and Large-Scale
744 Circulation. Cambridge University Press.
745 Vanneste, J. (2013). Balance and spontaneous wave generation in geophysical flows. In S. H.
746 Davis & P. Moin (Eds.), Annual Review of Fluid Mechanics, 45, 147-172).
747 von Storch, J. S., H. Sasaki, & Marotzke, J. (2007). Wind-generated power input to the deep
748 ocean: An estimate using a $ 1/10^o$ general circulation model.Journal of Physical Oceanog-
749 raphy, 37, 657-672.
750 Waterhouse, A. F., MacKinnon, J. A., Nash, J. D., Alford, M. H., Kunze, E., Simmons, H. L.,...
751 Lee, C. M. (2014). Global Patterns of Diapycnal Mixing from Measurements of the Turbulent
752 Dissipation Rate. Journal of Physical Oceanography, 44(7), 1854-1872. doi: 10.1175/Jpo-D-13-
753 0104.1
754
755 Watson, A. J., Ledwell, J. R., Messias, M.-J., King, B. A., Mackay, N., Meredith, M. P.,...
756 Naveira Garabato, A. C. (2013). Rapid cross-density ocean mixing at mid-depths in the Drake
757 Passage measured by tracer release. Nature, 501(7467), 408-411. doi: 10.1038/nature12432
758 Welander, P. (1955). Studies on the general development of motion in a 2-dimensional, ideal
759 fluid. Tellus, 7(2), 141-156.
760 Welander, P. (1971). The thermocline problem. Phil. Trans. Royal. Society London A, 270,
761 69-73.
762 Wunsch, C. (1970). On oceanic boundary mixing. Deep-sea Research, 17, 293-301.

763 Wunsch, C. (1972). Temperature microstructure on the Bermuda slope, with application to the
764 mean flow. Tellus, 24, 350-367.
765 Wyrtki, K. (1962). The oxygen minima in relation to ocean circulation. Deep-Sea Research,
766 9(1), 11-23.
767 Zhai, X. M., & Johnson, H. L., Marshall, D. P. (2010). Significant sink of ocean-eddy energy
768 near western boundaries. Nature Geoscience, 3(9), 608-612.